Microsc. Microanal. 22, 300–310, 2016
doi:10.1017/S143192761600012X

Microscopy AND Microanalysis

Quantitative Imaging of FRET-Based Biosensors for Cell- and Organelle-Specific Analyses in Plants

Swayoma Banerjee, Luis Rene Garcia, and Wayne K. Versaw*

Department of Biology, Texas A&M University, College Station, TX 77843, USA

Abstract: Genetically encoded Förster resonance energy transfer (FRET)-based biosensors have been used to report relative concentrations of ions and small molecules, as well as changes in protein conformation, posttranslational modifications, and protein–protein interactions. Changes in FRET are typically quantified through ratiometric analysis of fluorescence intensities. Here we describe methods to evaluate ratiometric imaging data acquired through confocal microscopy of a FRET-based inorganic phosphate biosensor in different cells and subcellular compartments of *Arabidopsis thaliana*. Linear regression was applied to donor, acceptor, and FRET-derived acceptor fluorescence intensities obtained from images of multiple plants to estimate FRET ratios and associated location-specific spectral correction factors with high precision. FRET/donor ratios provided a combination of high dynamic range and precision for this biosensor when applied to the cytosol of both root and leaf cells, but lower precision when this ratiometric method was applied to chloroplasts. We attribute this effect to quenching of donor fluorescence because high precision was achieved with FRET/acceptor ratios and thus is the preferred ratiometric method for this organelle. A ligand-insensitive biosensor was also used to distinguish nonspecific changes in FRET ratios. These studies provide a useful guide for conducting quantitative ratiometric studies in live plants that is applicable to any FRET-based biosensor.

Key words: biosensor, FRET, ratiometric, inorganic phosphate, Arabidopsis

Introduction

Genetically encoded Förster resonance energy transfer (FRET)-based biosensors are powerful tools for monitoring changes in the concentrations of ions and metabolites in live cells. The ability to analyze such changes with high spatiotemporal resolution has revolutionized studies of a myriad of cellular processes including transport, compartmentalization, signaling, and metabolism (Frommer et al., 2009; Okumoto et al., 2012; Jones et al., 2013). FRET biosensors for ions and small molecules consist of a ligand-binding domain fused to two spectral variants of green fluorescent protein (GFP), usually cyan fluorescent protein (CFP) and yellow fluorescent protein (YFP) variants. Ligand binding to such biosensors induces a conformational change that alters FRET efficiency, which is detected as a change in fluorescence lifetime (Hum et al., 2012) or, more commonly, through a change in the ratio of the intensities of the two fluorescent proteins, i.e., FRET ratio. Consequently, fluorescence lifetime and FRET ratio both reflect the fraction of biosensors in each conformation. This fraction is directly proportional to ligand concentration over a range that is defined by the binding affinity and ultimately, saturation of the biosensor.

FRET-based biosensors have been used more widely in animal cell systems than in plants, but there is a growing list of biosensors that have been developed or specifically adapted for use in plants that includes those for glucose, maltose, sucrose, glutamine, calcium, zinc, phosphate, and abscisic acid (Allen et al., 1999; Frommer et al., 2009; Okumoto et al., 2012; Gjetting et al., 2013; Jones et al., 2013, 2014; Waadt et al., 2014; Mukherjee et al., 2015). However, the successful application of FRET biosensors in plants has revealed a number of technical challenges. For example, RNA silencing severely limits expression and detection of some FRET biosensor transgenes (Deuschle et al., 2006). This problem was resolved through the use of an alternative promoter (Krebs et al., 2012), by limiting analyses to young seedlings (Rincon-Zachary et al., 2010; Chaudhuri et al., 2011), or by expressing the transgenes in RNA silencing mutants (Deuschle et al., 2006; Yang et al., 2010; Chaudhuri et al., 2011; Mukherjee et al., 2015).

Pigments and other endogenous molecules that contribute to either autofluorescence or the quenching of biosensor fluorescence also pose a challenge for quantitative studies in plants (Muller et al., 2013). Improvements in fluorescent proteins and in biosensor design, including the use of circularly permuted fluorescent proteins (Nagai et al., 2004; Krebs et al., 2012), have greatly increased both fluorescence intensities and dynamic range. Fluorescence quench, as well as variation in biosensor expression, can be partially resolved by using FRET sensitized emission, which accounts for donor spectral bleedthrough and acceptor cross-excitation to determine the fraction of acceptor fluorescence that is derived from FRET (Xia & Liu, 2001; Wallrabe & Periasamy, 2005; Okumoto, 2014). These corrections may be unnecessary if analyses are restricted to single cells, but could be critical when investigating ligand concentrations in different cell types or when comparing results from multiple individuals to ascertain gene/protein functions.

Received October 5, 2015; accepted January 13, 2016
*Corresponding author. wversaw@tamu.edu

Monitoring inorganic phosphate (Pi) in live plants is a particularly attractive application for FRET biosensors. The mechanisms underlying the systemic distribution of this essential nutrient are poorly understood yet cellular and subcellular concentrations are expected to vary in response to both environmental and metabolic conditions (Walker & Sivak, 1986; Raghothama, 1999; Vance et al., 2003; Plaxton & Tran, 2011; Kanno et al., 2012). Moreover, analytical methods that have been used previously to probe Pi contents of some plant cell compartments, such as nonaqueous fractionation and ^{31}P-NMR, lack cellular resolution (Rebeille et al., 1984; Sharkey & Vanderveer, 1989; Pratt et al., 2009; Gout et al., 2011). We recently adapted a Pi biosensor that had been used previously in animal cells (Gu et al., 2006) for use in plants (Mukherjee et al., 2015). The second-generation Pi biosensors, cpFLIPPi, consist of a cyanobacterial Pi binding protein fused between eCFP (FRET donor) and a circularly permuted Venus (cpVenus) (FRET acceptor). Ratiometric analyses with one of these biosensors, cpFLIPPi-6.4m, revealed changes in cytosolic Pi concentrations in root epidermal cells in response to varied external supply, and also allowed detection of a mutation-induced change in Pi accumulation within plastids in root epidermal cells. In both cases, the analyses relied on comparisons of pooled FRET/donor data.

In this study we expanded and refined our previous work by defining quantitative FRET ratiometric imaging methods for different cell types and subcellular compartments, including those with pigments. Specifically, we used confocal microscopy to image the cpFLIPPi-6.4m Pi biosensor in the cytosol of root epidermal cells and in both the cytosol and chloroplast stroma of leaf mesophyll cells of *Arabidopsis thaliana*. The application of linear regression to donor, acceptor, and FRET-derived acceptor fluorescence intensities for each target location in the plant improved the precision of estimates for FRET sensitized emission correction coefficients and for FRET ratios obtained from images of multiple plants. Our results also indicated that the FRET/eCFP ratio method is highly reproducible for the cytosol of both root and leaf cells, but is more variable when applied to chloroplasts. We attributed the variation to quenching of donor eCFP fluorescence by pigments within this organelle, but regardless of mechanism, the variation was largely eliminated when the FRET/cpVenus ratio method was applied to the same samples. Consequently, FRET/cpVenus (FRET/acceptor) is the preferred ratiometric method for FRET biosensors localized to chloroplasts.

Materials and Methods

Plasmids

Plasmids for expression of cpFLIPPi-6.4m in bacteria and in plants were described previously (Mukherjee et al., 2015). The cpFLIPPi-Null biosensor is a derivative of cpFLIPPi-6.4m in which a portion of the Pi binding domain has been altered from GAGAAF to ISGSTS. The cpFLIPPi-6.4m and cpFLIPPi-Null transgenes were cloned in pRSET for expression in *Escherichia coli* and in the pCN-UBQ10 plasmid (Mukherjee et al., 2015) for expression in Arabidopsis. Plastid-targeted variants of each sensor were constructed by inserting a 237 bp fragment encoding the 79-amino acid RbcS chloroplast transit peptide (Lee et al., 2006) in frame at the 5' end of the sensor genes.

In vitro Pi Binding Assays

The pRSET cpFLIPPi clones were introduced into *E. coli* BL21 (DE3) bacteria and single colonies were cultured overnight in 100 mL of Luria Bertani medium (Bertani, 1951). The cells were harvested by centrifugation and then lysed using BugBuster protein extraction reagents (EMD Millipore, Billerica, MA, USA). The expressed sensor proteins were purified from cell lysates using His-affinity chromatography with elution in 20 mM Tris-HCl, pH 7.5, 150 mM K-gluconate, and 400 mM imidazole. The eluent was dialyzed overnight at 4°C against 20 mM Tris-HCl, pH 7.5, then stored at 4°C. Protein concentration was quantified using the Bradford colorimetric assay and samples were diluted in protein dilution buffer: 100 mM K-gluconate, 30 mM NaCl, 25 mM MES, 25 mM HEPES, 40% (w/v) sucrose, pH 7.5. The protein solution was mixed with varied amounts of Pi, and the fluorescence was measured using a Synergy HT plate reader (Biotek, Winooski, VT, USA) with excitation at 420/27 nm and emission at both 485/20 nm (eCFP) and 540/25 nm (FRET-derived cpVenus). Excitation at 500/20 nm was used for direct excitation of cpVenus.

Generation of Transgenic Arabidopsis Plants

Cytosol- or plastid-targeted biosensor clones were introduced into *Agrobacterium tumefaciens* strain GV3101, and the resulting strains were used to transform Arabidopsis via the floral dip procedure (Clough & Bent, 1998). Transgenic plants were selected on agar medium containing 10 μM phosphinothricin. At least ten independent lines for each construct were examined for fluorescence and progeny from a representative line that maintained uniform fluorescence in the T2 generation were used for all subsequent studies.

Live Imaging of Roots and Leaves

For analysis of roots, Arabidopsis seeds were germinated and grown in 96-well microplates with 230 μL of 0.5 × Murashige and Skoog medium (Murashige & Skoog, 1962) containing 0.25% (w/v) sucrose and 250 μM Pi in a growth chamber (60% relative humidity, 21°C, and 90 μmol/m^2/s light intensity for a 16 h photoperiod.). After 5 days the seedlings were transferred to fresh medium containing either 250 μM Pi (Pi replete) or 10 μM Pi (Pi deficient). The media were replaced every 24 h. After 48 h seedlings were mounted in their respective growth medium on a cover glass, they were gently covered with a small cover glass to keep the roots flat when imaged using an inverted Olympus IX81 microscope equipped with a Yokogawa CSU-X1 Spinning Disk confocal unit and an iXon3 897 EMCCD camera (Andor Technology, Concord,

MA, USA). The same camera settings for electron-multiplying (EM) gain (5%) and preamplifier gain (2.4%) were used for all experiments. Plants were imaged using a 40× (numerical aperture 1.3) oil immersion objective. Comparable results were obtained in trial experiments using a 60× (numerical aperture 1.2) water immersion objective provided that all control images were captured with the same objective. A 445 nm laser was used to excite eCFP. A 483/32 nm filter was used to detect eCFP emission, and a 542/27 nm filter was used to detect FRET-derived cpVenus emission (FRET emission) and emission from directly excited cpVenus. A 515 nm laser was used for direct excitation of cpVenus.

For analysis of leaves, Arabidopsis plants were grown in soil for 4 weeks in a growth chamber with the same environmental conditions described above. The 5th rosette leaf was detached and immediately placed adaxial surface down in a custom made chamber (http:// microscopy.tamu.edu/lab-protocols/light-microscopy-protocols.html). The leaf was treated with perfluorodecalin to rapidly infiltrate intercellular air spaces and thereby improve optical qualities of the leaf (Littlejohn et al., 2010). This treatment had no measurable effect on biosensor fluorescence or FRET compared with water-mounted leaves. The leaf was gently covered with a small glass brick to keep the specimen flat against the cover glass. Palisade mesophyll cells were imaged using a 40× objective as described above. Untransformed plants were imaged using the same image acquisition setting to determine background fluorescence values.

Image Processing and Ratiometric FRET Analysis

Images were processed and analyzed using Metamorph and ImageJ software. Background fluorescence values (mean pixel intensities) for each combination of excitation and emission were determined for each target location in plants from images of five to ten cells in three to five untransformed plants. The mean background values for each emission channel were subtracted from the corresponding images of transgenic plants before further processing. Metamorph software was used to align the pixels for each emission channel to ensure that they were in register. A threshold was applied to each eCFP image because in all cases it had lower pixel intensities than the corresponding FRET emission and cpVenus images and thus specified the most restrictive boundary for the target location. A masked binary file was then created from the eCFP thresholded image. This binary file was multiplied to each of the three background-subtracted images for eCFP, FRET emission, and direct cpVenus, respectively. Regions of interest (ROIs) were applied to the eCFP image and mean intensity values for each ROI were recorded. The same ROIs were propagated to the FRET emission and direct cpVenus images, and mean intensities were recorded.

The FRET emission intensity values were corrected for donor spectral bleedthrough and acceptor cross-excitation to yield sensitized FRET emission values. Correction coefficients for spectral bleedthrough and cross-excitation were determined for each target cell compartment from images of plants expressing a single fluorescent protein (eCFP or cpVenus) using the same image acquisition settings used for biosensor imaging. Mean intensity values for ROIs applied to FRET emission images were plotted against the corresponding eCFP and direct cpVenus values. Linear regression using the LINEST function of Microsoft Excel™ v15.0 was applied to the data. The slopes of the fitted straight lines from FRET emission versus eCFP, and FRET emission versus direct cpVenus represent the donor spectral bleedthrough and acceptor cross-excitation correction coefficients, respectively. Sensitized FRET was calculated for each FRET emission ROI using the following equation: Sensitized FRET = Raw FRET − (eCFP emission × a) − (cpVenus emission × b), where a and b represent the donor spectral bleedthrough and acceptor cross-excitation factors, respectively.

Sensitized FRET/eCFP and sensitized FRET/cpVenus FRET ratios were calculated for each ROI then pooled to calculate mean values. Alternatively, sensitized FRET emission intensity values for all ROIs in a given cellular location were plotted separately against all of the corresponding eCFP and direct cpVenus intensity values, and then linear regression using the LINEST function of Microsoft Excel™ v15.0 was applied to the data. The slopes of the lines from these plots represent the fitted FRET/eCFP and fitted FRET/cpVenus ratio, respectively.

Results and Discussion

Defined Image Acquisition for Different Cell Types and Subcellular Compartments

Pi is an essential nutrient with key structural and regulatory roles that impinge on nearly every facet of plant growth and metabolism (Vance et al., 2003; Plaxton & Tran, 2011). However, our understanding of the mechanisms underlying Pi distribution and compartmentalization throughout the plant, as well as those required for the sensing and signaling of its availability (Chiou & Lin, 2011; Zhang et al., 2014), are limited by the inability to monitor Pi concentrations in individual cells and subcellular compartments of live plants. We demonstrated recently that ratiometric imaging of a Pi biosensor could be used to detect changes in Pi concentrations within the cytosol and plastids of root epidermal cells (Mukherjee et al., 2015). We therefore wished to expand this approach to other cell types and subcellular compartments as a step toward holistic studies of Pi homeostasis.

Previously, we could not be certain that the same imaging and/or analysis regimes could be applied to other cell types or organelles, particularly those that contain pigments. Indeed, fluorescence signals from the cpFLIPPi-6.4m Pi biosensor were much weaker in mature leaves than in seedling roots when the same imaging conditions were used. We therefore sought to optimize image capture settings for each of our target cellular and subcellular locations. Although our efforts focused on cpFLIPPi-6.4m, we suggest that the overall strategy and associated considerations are broadly applicable to other FRET biosensors.

An initial criterion for image capture optimization was to ensure that pixel intensities were well above background levels, yet also below saturation in each of the three images needed for ratiometric FRET analysis: eCFP (donor excitation and emission), FRET emission (donor excitation, acceptor emission), and direct cpVenus (acceptor excitation and emission). Another constraint was that for a given location in the plant, the same image capture settings were needed for eCFP and FRET emission to provide a quantitative measure of the ligand-dependent fluorescent outputs of the biosensor. The image capture variables for our confocal system included excitation laser intensity, exposure time, and camera sensitivity (EM gain and preamplifier gain). For convenience, we chose to use the same camera sensitivity settings for all experiments. In addition, because the EMCCD camera we used has a single detector, eCFP and FRET emission images were captured with equivalent sensitivity. However, it should be noted that if a confocal system is used that employs two or more detectors then the spectral responses and sensitivities of each detector must be defined independently for each experimental condition (van Rheenen et al., 2004). We varied laser intensities and exposure times to yield mean pixel intensities that were ~10-fold greater than those for background fluorescence measured with the same settings. This signal-to-background ratio ensured that all measurements were within the linear range of the camera, which was necessary for quantitative measurements (Brown, 2007).

Because direct cpVenus fluorescence reflects biosensor abundance rather than ligand concentration, arbitrary image capture settings could have been used provided that the pixel intensities fell within the linear range of the camera. However, we chose to use settings that yielded mean pixel intensity values similar to those for eCFP and FRET emission because this minimized any potential variations in detector sensitivity. This was an important consideration since direct cpVenus fluorescence was used to determine FRET sensitized emission values and, in some cases, was used to normalize FRET emission (described in the following sections).

Images captured with optimized settings required processing before ratiometric analyses could be conducted. Figure 1 illustrates the image processing steps used in this study. First, background fluorescence was removed from raw images by subtracting mean pixel intensities obtained from images of the same locations in untransformed plants (Fig. 1a). A threshold was then manually applied to eCFP images to define the boundaries of the biosensor location (Fig. 1b). The eCFP images were chosen for this step because they consistently had the lowest pixel intensity value and would therefore provide the most conservative boundaries. To apply the same boundaries to the corresponding FRET emission and direct cpVenus images, the thresholded eCFP image was first converted to a masked binary image file (Fig. 1b). This step converted all of the fluorescence intensities above the threshold in the eCFP image to a value of one, and all intensities below the threshold to zero. The values for each pixel in the masked binary image were then multiplied to the corresponding pixel intensities in the background-subtracted eCFP, FRET emission, and direct cpVenus images to yield final processed images (Fig. 1c). ROIs were applied to the processed images (Fig. 1c), and mean pixel intensities for all pixels with intensities greater than zero within each ROI were recorded.

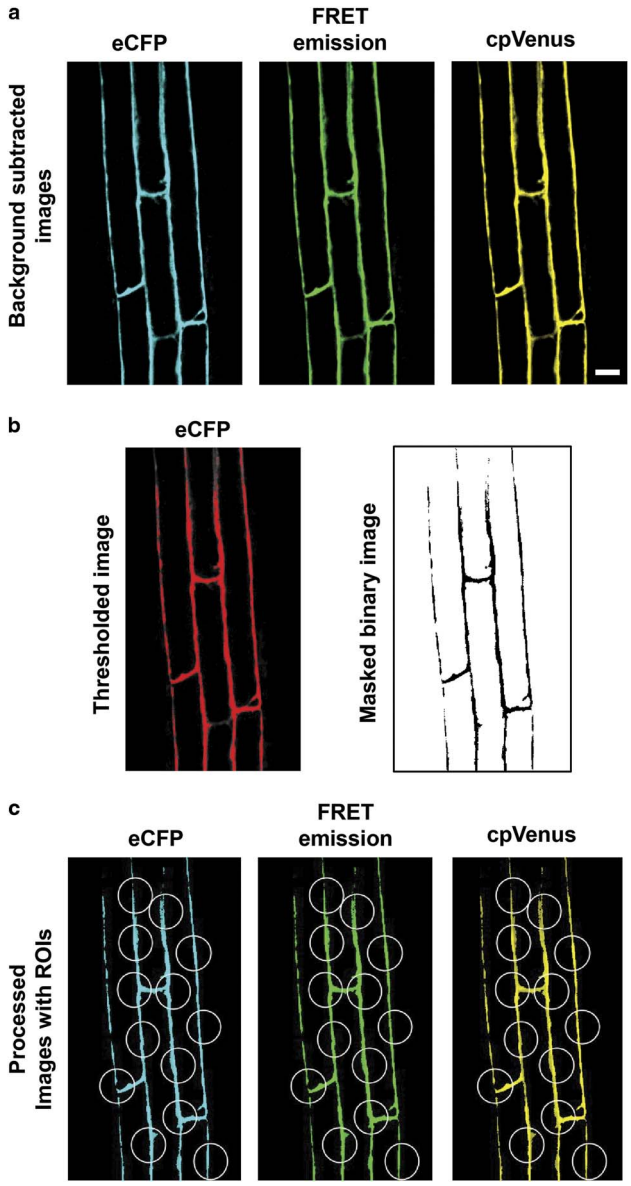

Figure 1. Stages of image processing. **a:** Images for eCFP, FRET emission, and direct cpVenus after background subtraction. **b:** Threshold applied to an eCFP image and the masked binary image (black and white) created from the thresholded eCFP image. **c:** Final processed eCFP, FRET emission, and cpVenus images. Regions of interest (ROIs) are drawn on the final images. Scale bar is 10 μm. FRET, Förster resonance energy transfer.

Location-Specific Spectral Correction Coefficients

We wanted to use the FRET ratio as the readout of relative Pi levels in different locations in the plant, but first needed to

evaluate spectral factors that could influence ratio values. For example, donor bleedthrough (eCFP fluorescence that is detected in the cpVenus channel) and acceptor cross-excitation (direct excitation of cpVenus by the eCFP excitation laser) could vary with biosensor expression and/or cellular location (Xia & Liu, 2001; Day & Davidson, 2012). We first assessed the extent that bleedthrough and cross-excitation varied with fluorescence intensity and then determined spectral correction coefficients that we could use to correct for their respective contributions to FRET emission in each of our target locations, i.e., to calculate FRET sensitized emission. From six to eight independent plants expressing either eCFP (donor alone) or cpVenus (acceptor alone), we captured and processed eCFP, FRET emission, and direct cpVenus images for cytosol of root epidermal cells and for cytosol and chloroplast stroma of leaf palisade mesophyll cells. All images were captured using the same optimized settings used to image cpFLIPPi-6.4m. ROIs were applied to these images and mean pixel intensities were recorded.

Fluorescence intensity values varied up to ninefold in some cases (Fig. 2). However, plots of eCFP bleedthrough versus eCFP, and of cpVenus cross-excitation versus direct cpVenus revealed that both bleedthrough (Figs. 2a, 2c, 2e) and cross-excitation (Figs. 2b, 2d, 2f) were directly proportional to fluorescence intensity over the entire range of intensities detected in each of the locations we examined.

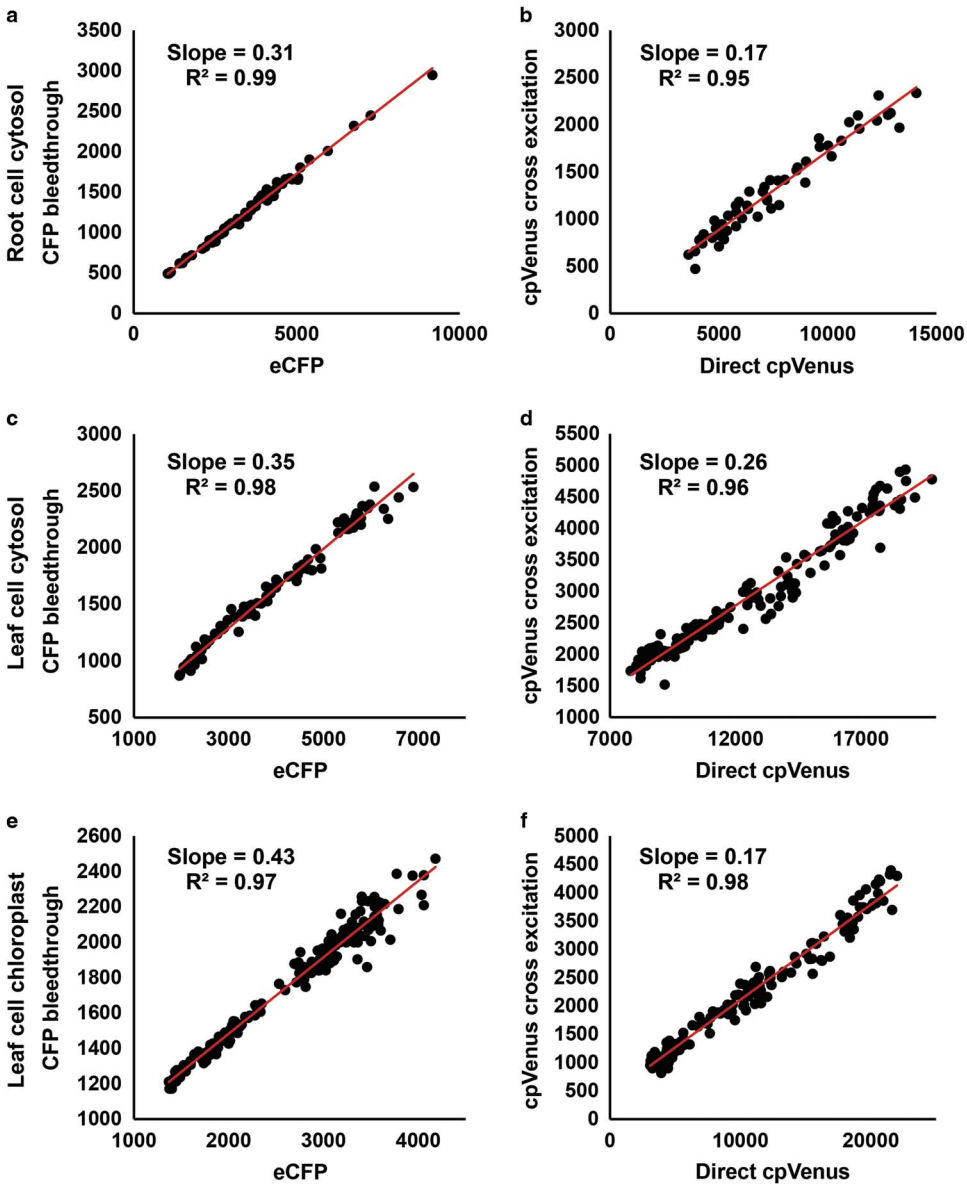

Figure 2. Determination of location-specific FRET correction coefficients. Mean intensity values obtained from 15 to 20 ROIs in FRET emission images from six to eight independent plants are plotted against the corresponding intensity values from eCFP or direct cpVenus images. Slopes of the graphs represent correction coefficients for donor bleedthrough and acceptor cross-excitation that were used to calculate FRET sensitized emission. FRET, Förster resonance energy transfer; ROIs, regions of interest.

Consequently, we applied linear regression to data in each plot to yield a fitted line with a slope that represents a spectral correction coefficient. That is, slopes in Figures 2a, 2c, and 2e are the coefficients for correcting eCFP bleedthrough, and slopes in Figures 2b, 2d, and 2f are the coefficients for correcting acceptor cpVenus cross-excitation.

We could have calculated correction coefficients from the mean of pooled FRET ratio values (bleedthrough/eCFP and cross-excitation/direct cpVenus), but this would have been a source of error for subsequent ratiometric FRET analyses if one or both fluorescence responses had been nonlinear. In such an event, nonlinear regression would have been used to derive the coefficients. Alternatively, plugins for ImageJ are available to calculate nonlinear coefficients (Feige et al., 2005; Roszik et al., 2009), but plotting intensity values from multiple individuals as described here provided a simple way to assess data variation within a population.

Although donor bleedthrough and acceptor cross-excitation were uniformly proportional to fluorescence intensity within a given location in the plant, the corresponding correction coefficients differed between locations. We hypothesize that these differences reflect consistent differences in the chemical environments of each location, such as concentrations of pigments or other molecules that could influence, e.g., quench, the fluorescence of one or both of the fluorescent proteins. Regardless of the underlying mechanism, our results indicate that location-specific spectral correction coefficients must be defined to accurately assess biosensor FRET ratios in different cell compartments. Accordingly, all FRET emission data described hereafter were corrected using location-matched correction coefficients to yield FRET sensitized emission.

Ratiometric FRET Analyses: FRET/Donor Versus FRET/Acceptor

Although several ratiometric FRET analysis methods have been described (Xia & Liu, 2001; Feige et al., 2005), the FRET/donor ratio method is most commonly employed because it is highly sensitive to changes in ligand concentration. With this method, fluorescence intensities of the numerator and denominator components of the ratio both change in response to ligand concentration, and the changes are in opposite directions, thus yielding a large response. However, we hypothesized that the FRET/acceptor ratio would be preferable when examining pigmented cells/cell compartments. Our rationale was that pigments would affect eCFP and cpVenus fluorescence unequally, primarily because chlorophyll absorbs light over a broad range (400–500 nm) that coincides with eCFP emission. As a result, eCFP fluorescence could be quenched. However, because FRET emission and acceptor both rely on output from cpVenus, any effects of pigments on its fluorescence would be proportional. Chlorophyll fluorescence occurs at wavelengths greater than 600 nm so would have a negligible effect on quantitation of either eCFP or cpVenus fluorescence.

To systematically compare the efficacies of FRET/donor and FRET/acceptor approaches for different cellular locations we imaged plants expressing the cpFLIPPi-6.4m Pi biosensor using location-specific image capture settings and processed the images as described in Figure 1. We then used the corresponding location-specific spectral corrections coefficients (Fig. 2) to calculate FRET sensitized emission [Sensitized FRET = Raw FRET – (eCFP emission × eCFP bleedthrough) – (cpVenus emission × cpVenus cross-excitation)]. We first compared the two FRET ratio analysis methods for the cytosol of root epidermal and leaf palisade mesophyll cells (Fig. 3). Pigments do not typically accumulate in the cytosol, but we could not know if pigments, particularly chlorophyll, present in other parts of the leaf would affect donor or acceptor fluorescence unequally. Fluorescence intensities varied by up to fivefold in some cases, but plots of FRET emission versus eCFP (Figs. 3a, 3c) and of FRET emission versus direct cpVenus (Figs. 3b, 3d) showed that FRET emission was directly proportional to both donor and acceptor emission in both cell types, as required for ratiometric analysis.

As with the derivation of spectral correction coefficients, FRET ratios could be calculated in two ways. One was to determine the desired FRET ratio for each ROI in a given location and to then calculate the pooled mean. Alternatively, linear regression could be applied to the data in each plot, and the slope of the fitted line would represent the FRET ratio for the population. We compared results from both of these calculation approaches as part of our comparison of FRET ratio methods. As shown in Table 1, relative errors for measurements of FRET/eCFP were consistently lower than those for FRET/cpVenus in the same cell type, and in all cases the relative errors for measurements obtained through linear regression were substantially lower than when using pooled values. We therefore conclude that FRET/eCFP (FRET/donor) is the preferred ratiometric method for the cytosol of both root and leaf cells, and that the use of linear regression provides a more precise estimate of the FRET ratio for a population.

It should be noted that the use of linear regression to improve estimates of the FRET ratio is limited to situations where a relatively wide distribution of fluorescence intensities exists, which is typical for analyses involving multiple plants. When fluorescence intensities are largely invariant, as might be expected when repeatedly imaging a single cell, then the use of linear regression would be unnecessary, and this conclusion would be supported through comparison of relative errors. For example, we found that FRET ratios within a field of view, as depicted in Figures 3e, 3f and 4c, varied by <4%. Regardless of whether linear regression is used, plotting FRET emission versus donor or acceptor fluorescence would allow rapid evaluation of the population data set to identify individuals with attributes outside the population norm, which may be particularly important when evaluating the effects of environmental conditions or pleiotropic mutations.

In contrast to our recommendation for the cytosol, FRET/acceptor rather than FRET/donor should be used

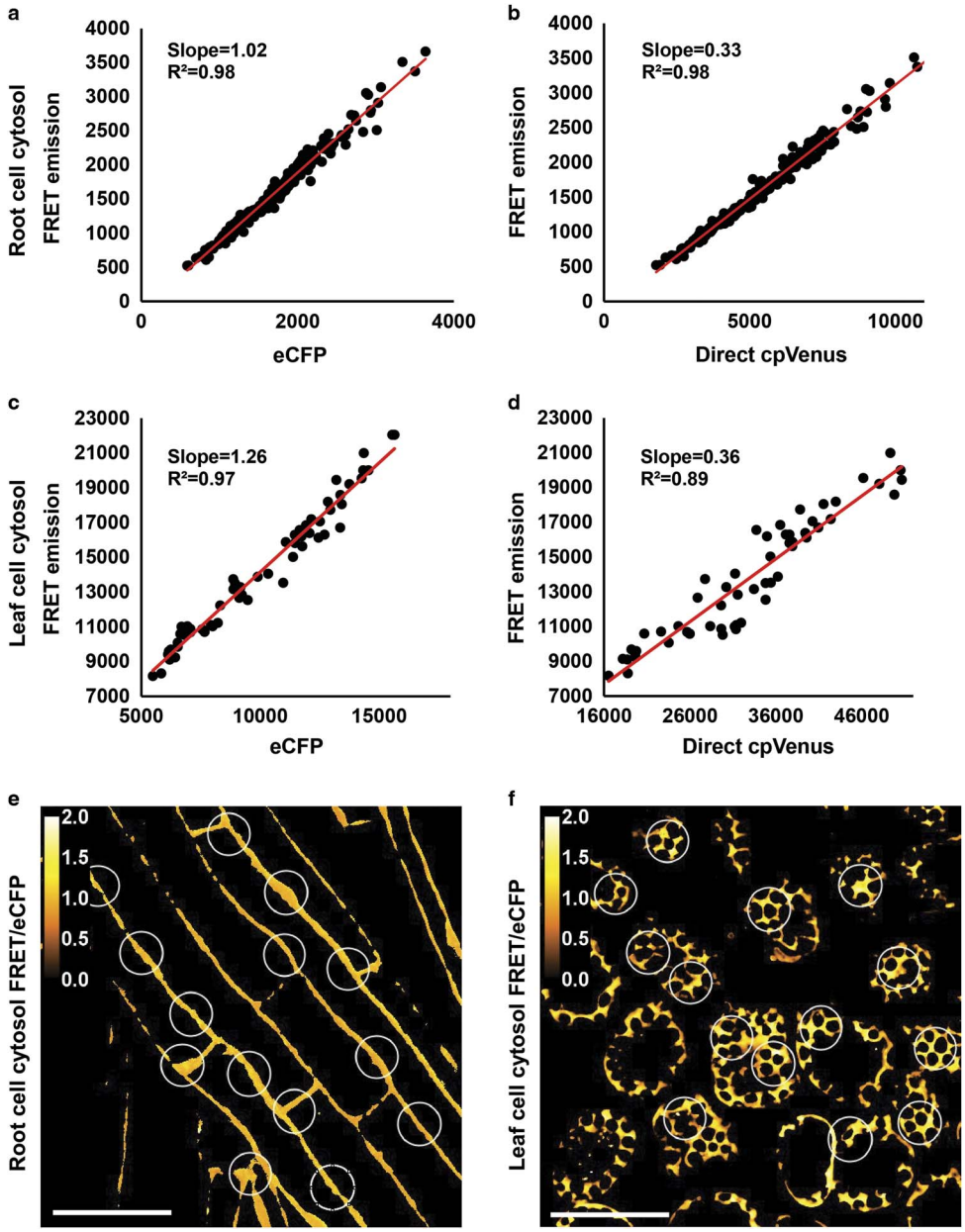

Figure 3. Ratiometric FRET analysis in cytosol. **a–d:** Plots of FRET sensitized emission versus either eCFP or direct cpVenus mean intensity values obtained from 15 to 20 ROIs in the corresponding image files. Trend lines were determined from linear regression. Slopes represent fitted mean FRET ratios. Each plot includes data from six to eight independent plants. **e, f:** Representative pseudo-colored FRET ratio images were generated by dividing FRET emission pixel intensity values by eCFP pixel intensity values. Color bars indicate the range of FRET/eCFP ratios in the cytosol of root epidermal and leaf mesophyll cells. Scale bar is 50 μm. FRET, Förster resonance energy transfer; ROIs, regions of interest.

when analyzing biosensors localized to chloroplasts. FRET emission was proportional to eCFP (Fig. 4a), but the data points were more widely scattered than those for cytosol (Fig. 3) and, as expected, the relative error was high even when linear regression was used (Table 1). It was possible that the variation in FRET/eCFP reflected heterogeneity of Pi concentrations between chloroplasts. However, this possibility was rejected because the variation was largely eliminated when we examined FRET/cpVenus (Fig. 4b) and the relative error was equivalent to those for measurements in the cytosol (Table 1). These results support our hypothesis that pigments or some other aspect of the local environment within chloroplasts affect eCFP and cpVenus unequally. Regardless of the basis for this effect it can be overcome by normalizing FRET emission values to cpVenus intensity. Although FRET/acceptor is less sensitive to changes in ligand concentration than FRET/donor because only the numerator is responsive to Pi concentration, the increase in precision (reduced relative error) is a desirable compromise that would facilitate detection of subtle changes in Pi concentrations.

Table 1. Comparison of FRET Ratio Analysis Methods for Different Cellular and Subcellular Locations.

Biosensor	Organ	Cell Type	Subcellular Location	FRET Ratio Method	FRET Ratio from Pooled ROIs (mean ± SD, % relative error)	FRET Ratio from Linear Regression (mean ± SD, % relative error)
cpFLIPPi-6.4m	Root	Epidermis	Cytosol	FRET/eCFP	0.92 ± 0.06, 6.5	1.02 ± 0.02, 2.0
cpFLIPPi-6.4m	Root	Epidermis	Cytosol	FRET/cpVenus	0.29 ± 0.02, 6.9	0.32 ± 0.003, 0.9
cpFLIPPi-6.4m	Leaf	Mesophyll	Cytosol	FRET/eCFP	1.43 ± 0.09, 6.2	1.26 ± 0.03, 2.3
cpFLIPPi-6.4m	Leaf	Mesophyll	Cytosol	FRET/cpVenus	0.42 ± 0.04, 10.4	0.36 ± 0.02, 4.7
cpFLIPPi-6.4m	Leaf	Mesophyll	Chloroplast	FRET/eCFP	1.24 ± 0.24, 19.4	1.29 ± 0.09, 7.0
cpFLIPPi-6.4m	Leaf	Mesophyll	Chloroplast	FRET/cpVenus	0.61 ± 0.04, 6.6	0.60 ± 0.01, 1.7
cpFLIPPi-Null	Root	Epidermis	Cytosol	FRET/eCFP	0.65 ± 0.03, 3.8	0.72 ± 0.01, 1.6
cpFLIPPi-Null	Root	Epidermis	Cytosol	FRET/cpVenus	0.28 ± 0.01, 5.4	0.26 ± 0.007, 2.8
cpFLIPPi-Null	Leaf	Mesophyll	Cytosol	FRET/eCFP	0.87 ± 0.06, 7.3	0.90 ± 0.02, 2.4
cpFLIPPi-Null	Leaf	Mesophyll	Cytosol	FRET/cpVenus	0.49 ± 0.03, 7.0	0.50 ± 0.01, 2.4
cpFLIPPi-Null	Leaf	Mesophyll	Chloroplast	FRET/eCFP	0.85 ± 0.06, 7.3	0.91 ± 0.02, 2.4
cpFLIPPi-Null	Leaf	Mesophyll	Chloroplast	FRET/cpVenus	0.34 ± 0.03, 8.6	0.35 ± 0.01, 3.0

FRET, Förster resonance energy transfer; ROIs, regions of interest.

Substitution of the eCFP and cpVenus components of the Pi biosensor with red-shifted fluorescent proteins that support FRET, i.e. green and red variants (Lam et al., 2012), would minimize the potential effects of chlorophyll and other pigments. However, such substitutions often require extensive optimization to attain fluorophore orientations suitable to detect ligand-dependent changes in FRET (Miyawaki, 2003; Deuschle et al., 2005; Muller et al., 2013). Until such biosensors are available, the methods described here for blue–yellow FRET pairs remain broadly applicable.

Using a Ligand-Insensitive Biosensor to Distinguish Nonspecific Changes in FRET Ratios

Even when FRET ratios are carefully defined a control is needed to distinguish what fraction of any observed differences are due to ligand-independent parameters, which could include pH and various ion concentrations, particularly chloride (Shaner et al., 2005). Differences in such nonspecific factors may be inherent or a consequence of experimental treatment. We previously used a cpFLIPPi variant with high affinity for Pi as a control for nonspecific changes in FRET/eCFP ratios (Mukherjee et al., 2015). However, we could not be certain that this biosensor variant would be saturated in all cellular contexts. We therefore isolated a Pi-insensitive variant, cpFLIPPi-Null, from a mutant library that was described previously (Mukherjee et al., 2015). We confirmed that cpFLIPPi-Null was insensitive to Pi concentration using an *in vitro* binding assay in which cpFLIPPi-6.4m yielded the expected Pi-dependent decrease in FRET/eCFP ratio (Fig. 5).

As shown in Fig. 5a, cpFLIPPi-Null yielded lower FRET/eCFP ratio values than cpFLIPPi-6.4m even in the absence of Pi. This difference in absolute FRET ratio most likely reflects the relative orientations of the fluorophores (Deuschle et al., 2005), which is an unavoidable and largely arbitrary consequence of the small differences in protein sequences. However, normalization of FRET ratios allows direct comparisons between biosensor responses (Keinath et al., 2015). For example, the relative effects of Pi concentration on the two biosensors is shown in Figure 5b. Importantly, this approach can also be applied to assess the effects of nonspecific factors on the FRET ratio. For example, changes in pH and chloride concentration both affected the FRET ratio, but the relative effects were equivalent for cpFLIPPi-6.4m and cpFLIPPi-Null (Fig. 6), indicating that cpFLIPPi-Null is a suitable control for distinguishing nonspecific changes in the FRET ratio.

The cpFLIPPi-Null biosensor control was expressed in Arabidopsis plants and images were captured and processed for each target location exactly as described for cpFLIPPi-6.4m. FRET ratio values for each location (Table 1) were then used to distinguish Pi-specific from nonspecific changes in FRET ratios. For example, we wanted to know what fraction of the difference between FRET/eCFP ratio for cpFLIPPi-6.4m in the cytosol of leaf mesophyll (1.26) and root epidermis (1.02) was due to Pi concentration given that FRET/eCFP values for cpFLIPPi-Null also differed in these locations, 0.9 for mesophyll and 0.72 for root epidermis. To compare these differences we calculated relative changes for each biosensor. Specifically, the FRET/eCFP ratio for cpFLPPI-6.4m was 23.5% greater in the cytosol of leaf mesophyll than root epidermis, whereas cpFLIPPi-Null exhibited a 25% difference between the same locations suggesting that none of the difference observed with cpFLIPPi-6.4m could be attributed to Pi.

We also used cpFLIPPi-Null to evaluate changes in the FRET ratio associated with experimental treatment. In this case we examined the effect of Pi deprivation on the FRET/eCFP ratio measured in the cytosol of root epidermal cells. Again, FRET ratios for both cpFLIPPi-6.4m and cpFLIPPi-Null increased (Fig. 7), which for cpFLIPPi-6.4m would be consistent with an expected decrease in Pi concentration. The FRET ratio for cpFLIPPi-6.4m increased 45%, whereas the FRET ratio for cpFLIPPi-Null increased only 17%. Thus, the 17% change observed for cpFLIPPi-Null represents nonspecific

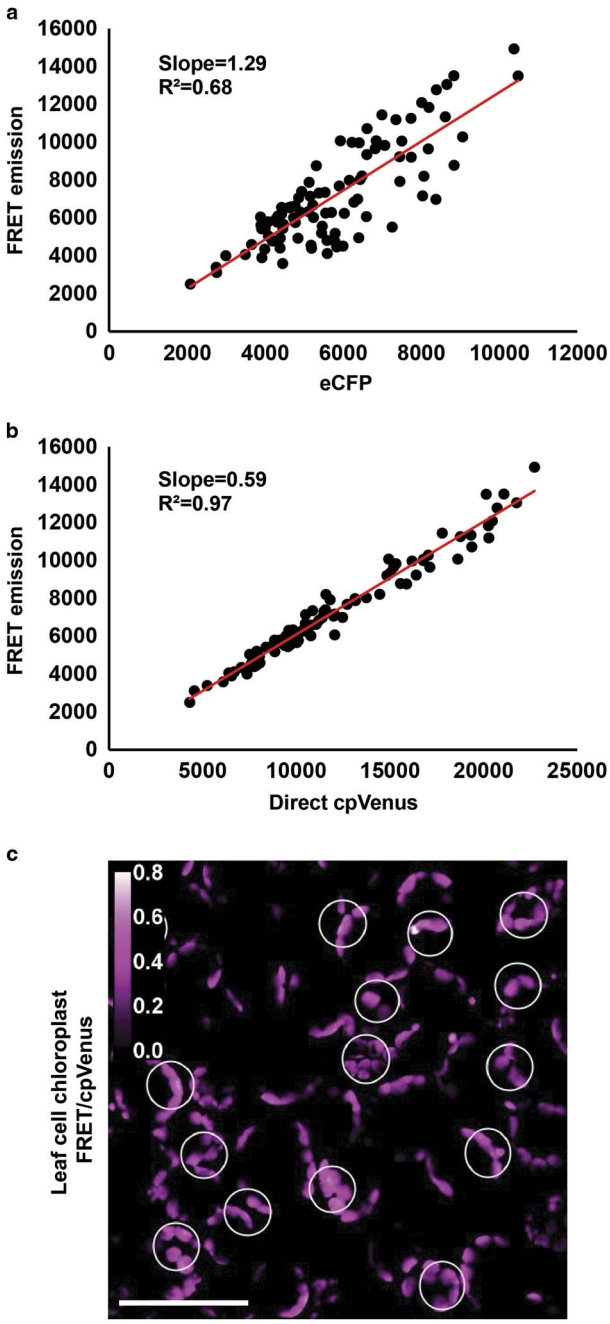

Figure 4. Ratiometric FRET analysis in chloroplasts. Plots of FRET sensitized emission versus eCFP (**a**) and direct cpVenus (**b**) mean intensity values obtained from 15 to 20 ROIs in each of six to eight independent plants. Trend lines were determined from linear regression. Slopes represent fitted mean FRET ratios. **c:** Representative pseudo-colored FRET ratio images were generated by dividing FRET emission pixel intensity values by cpVenus pixel intensity values. Color bar indicates the range of FRET/cpVenus ratios in chloroplasts within leaf mesophyll cells. Scale bar is 50 μm. FRET, Förster resonance energy transfer; ROIs, regions of interest.

changes in the cytosol associated with the Pi deprivation treatment. Taking account of this nonspecific effect, 28% of the change in the FRET/eCFP ratio for cpFLIPPi-6.4m can be attributed to a decrease in Pi concentration.

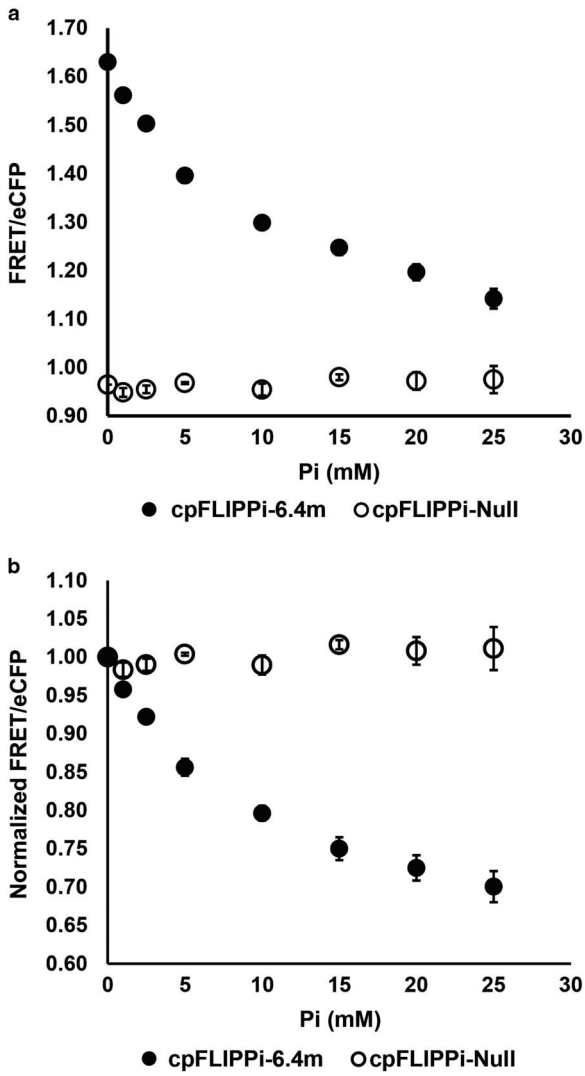

Figure 5. Comparisons of FRET/eCFP responses for cpFLIPPi-6.4m and cpFLIPPi-Null *in vitro*. **a:** Effect of Pi concentration on FRET/eCFP ratios for purified cpFLIPPi-6.4m and cpFLIPPi-Null in an *in vitro* assay. Values shown are mean ± standard deviation for three replicates. **b:** Effect of Pi concentration on normalized FRET/eCFP ratios from the same data shown in (**a**). Values were normalized to the FRET/eCFP ratio measured in the absence of Pi. FRET, Förster resonance energy transfer.

Summary

Although optimal image capture settings must be determined empirically for every combination of biosensor, microscope, camera, and cellular location, we have described approaches to facilitate optimization of these parameters for quantitative analysis of genetically encoded FRET biosensors using confocal microscopy. These approaches are applicable to any FRET biosensor. The application of linear regression to fluorescence data to obtain FRET ratio values is particularly useful when multiple individuals that exhibit a range of fluorescence intensities are used because the increased precision enhances the ability to detect small differences in ligand concentration. This may be critical when comparing

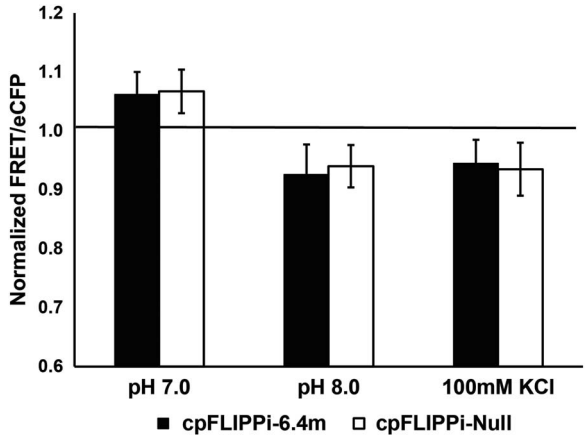

Figure 6. Effect of nonspecific factors on FRET/eCFP ratio for cpFLIPPi-6.4m and cpFLIPPi-Null. FRET/eCFP ratios were measured for purified biosensor proteins using an *in vitro* assay in which pH or KCl concentration was altered as indicated. Values were normalized to those obtained with the standard assay condition (pH 7.5, 0 mM KCl), which are indicated by the black line. Values shown are mean ± standard deviation for three replicates. FRET, Förster resonance energy transfer.

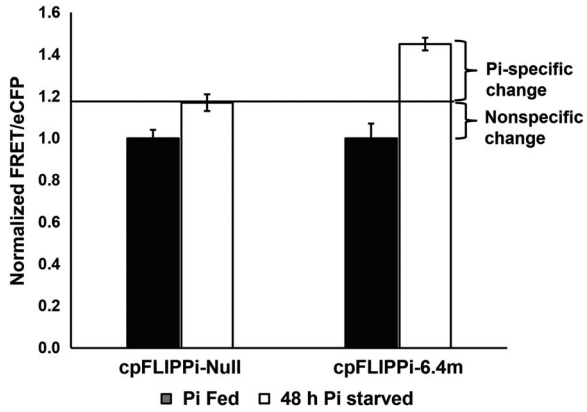

Figure 7. Effect of Pi deprivation on normalized FRET/eCFP ratios for the cytosol of root epidermal cells. Seedlings expressing cpFLIPPi-6.4m or cpFLIPPi-Null were maintained in Pi-fed growth conditions or deprived of Pi for 48 h before imaging. FRET/eCFP values from Pi-fed seedlings were used for normalization. Values shown are mean ± standard deviation for six independent seedlings ($p < 0.001$, Student's t test). FRET, Förster resonance energy transfer.

populations with different genotypes to discern gene/protein function. The increase in precision also applies to the choice of normalizer for FRET sensitized emission. FRET/eCFP is preferred when the biosensor is localized to the cytosol. In contrast, FRET/cpVenus is recommended when the biosensor is localized to chloroplasts. It must be emphasized that the ratiometric approaches we have described report relative changes in ligand concentration. Calibration must be established to define absolute ligand concentrations. Ideally, calibrations would involve direct manipulation of ligand concentrations in the target location, e.g., via microinjection, but this is technically challenging and may not be achievable for some subcellular compartments. Alternative approaches include *in situ* calibrations, which can be conducted when the ligand and/or chelators readily diffuse across cell membranes, and *in vitro* calibrations using purified proteins suspended in solutions that mimic the target cell compartment as closely as possible. The continued development of calibration strategies will be needed to enable broad comparisons of results with FRET biosensors.

Acknowledgments

This work was supported by the National Science Foundation (grant no. IOS-0956486 to W.K.V.), the Department of Energy (grant no. DE-SC0014037 to W.K.V.), and the Howard Hughes Medical Institute (L.R.G.).

References

Allen, G.J., Kwak, J.M., Chu, S.P., Llopis, J., Tsien, R.Y., Harper, J.F. & Schroeder, J.I. (1999). Cameleon calcium indicator reports cytoplasmic calcium dynamics in Arabidopsis guard cells. *Plant J* **19**(6), 735–747.

Bertani, G. (1951). Studies on lysogenesis. I. The mode of phage liberation by lysogenic. *Escherichia coli. J Bacteriol* **62**(8), 293–300.

Brown, C.M. (2007). Fluorescence microscopy—Avoiding the pitfalls. *J Cell Sci* **120**(10), 1703–1705.

Chaudhuri, B., Hormann, F. & Frommer, W.B. (2011). Dynamic imaging of glucose flux impedance using FRET sensors in wild-type Arabidopsis plants. *J Exp Bot* **62**(7), 2411–2417.

Chiou, T.J. & Lin, S.I. (2011). Signaling network in sensing phosphate availability in plants. *Annu Rev Plant Biol* **62**, 185–206.

Clough, S.J. & Bent, A.F. (1998). Floral dip: A simplified method for Agrobacterium-mediated transformation of *Arabidopsis thaliana*. *Plant J* **16**(6), 735–743.

Day, R.N. & Davidson, M.W. (2012). Fluorescent proteins for FRET microscopy: Monitoring protein interactions in living cells. *Bioessays* **34**(5), 341–350.

Deuschle, K., Chaudhuri, B., Okumoto, S., Lager, I., Lalonde, S. & Frommer, W.B. (2006). Rapid metabolism of glucose detected with FRET glucose nanosensors in epidermal cells and intact roots of Arabidopsis RNA-silencing mutants. *Plant Cell* **18**(9), 2314–2325.

Deuschle, K., Okumoto, S., Fehr, M., Looger, L.L., Kozhukh, L. & Frommer, W.B. (2005). Construction and optimization of a family of genetically encoded metabolite sensors by semirational protein engineering. *Protein Sci* **14**(9), 2304–2314.

Feige, J.N., Sage, D., Wahli, W., Desvergne, B. & Gelman, L. (2005). PixFRET, an ImageJ plug-in for FRET calculation that can accommodate variations in spectral bleed-throughs. *Microsc Res Tech* **68**(1), 51–58.

Frommer, W.B., Davidson, M.W. & Campbell, R.E. (2009). Genetically encoded biosensors based on engineered fluorescent proteins. *Chem Soc Rev* **38**(10), 2833–2841.

Gjetting, S.K., Schulz, A. & Fuglsang, A.T. (2013). Perspectives for using genetically encoded fluorescent biosensors in plants. *Front Plant Sci* **4**, 234. doi:210.3389/fpls.2013.00234.

Gout, E., Bligny, R., Douce, R., Boisson, A.M. & Rivasseau, C. (2011). Early response of plant cell to carbon deprivation: In vivo 31P-NMR spectroscopy shows a quasi-instantaneous disruption on cytosolic sugars, phosphorylated intermediates of energy metabolism, phosphate partitioning, and intracellular pHs. *New Phytol* **189**(1), 135–147.

Gu, H., Lalonde, S., Okumoto, S., Looger, L.L., Scharff-Poulsen, A. M., Grossman, A.R., Kossmann, J., Jakobsen, I. & Frommer, W.B. (2006). A novel analytical method for in vivo phosphate tracking. *FEBS Lett* **580**(25), 5885–5893.

Hum, J.M., Siegel, A.P., Pavalko, F.M. & Day, R.N. (2012). Monitoring biosensor activity in living cells with fluorescence lifetime imaging microscopy. *Int J Mol Sci* **13**(11), 14385–14400.

Jones, A.M., Danielson, J.A., Manojkumar, S.N., Lanquar, V., Grossmann, G. & Frommer, W.B. (2014). Abscisic acid dynamics in roots detected with genetically encoded FRET sensors. *Elife* **3**, e01741.

Jones, A.M., Grossmann, G., Danielson, J.A., Sosso, D., Chen, L.Q., Ho, C.H. & Frommer, W.B. (2013). In vivo biochemistry: Applications for small molecule biosensors in plant biology. *Curr Opin Plant Biol* **16**(3), 389–395.

Kanno, S., Yamawaki, M., Ishibashi, H., Kobayashi, N.I., Hirose, A., Tanoi, K., Nussaume, L. & Nakanishi, T.M. (2012). Development of real-time radioisotope imaging systems for plant nutrient uptake studies. *Philos Trans R Soc Lond B Biol Sci* **367**(1595), 1501–1508.

Keinath, N.F., Waadt, R., Brugman, R., Schroeder, J.I., Grossmann, G., Schumacher, K. & Krebs, M. (2015). Live cell imaging with R-GECO1 sheds light on flg22- and chitin-induced transient [Ca(2+)]cyt patterns in Arabidopsis. *Mol Plant* **8**(8), 1188–1200.

Krebs, M., Held, K., Binder, A., Hashimoto, K., Den Herder, G., Parniske, M., Kudla, J. & Schumacher, K. (2012). FRET-based genetically encoded sensors allow high-resolution live cell imaging of Ca(2)(+) dynamics. *Plant J* **69**(1), 181–192.

Lam, A.J., St-Pierre, F., Gong, Y., Marshall, J.D., Cranfill, P.J., Baird, M.A., McKeown, M.R., Wiedenmann, J., Davidson, M.W., Schnitzer, M.J., Tsien, R.Y. & Lin, M.Z. (2012). Improving FRET dynamic range with bright green and red fluorescent proteins. *Nat Methods* **9**(10), 1005–1012.

Lee, D.W., Lee, S., Lee, G.-J., Lee, K.H., Kim, S., Cheong, G.-W. & Hwang, I. (2006). Functional characterization of sequence motifs in the transit peptide of Arabidopsis small subunit of rubisco. *Plant Physiol* **140**(2), 466–483.

Littlejohn, G.R., Gouveia, J.D., Edner, C., Smirnoff, N. & Love, J. (2010). Perfluorodecalin enhances in vivo confocal microscopy resolution of *Arabidopsis thaliana* mesophyll. *New Phytol* **186**(4), 1018–1025.

Miyawaki, A. (2003). Visualization of the spatial and temporal dynamics of intracellular signaling. *Dev Cell* **4**(3), 295–305.

Mukherjee, P., Banerjee, S., Wheeler, A., Ratliff, L.A., Irigoyen, S., Garcia, L.R., Lockless, S.W. & Versaw, W.K. (2015). Live imaging of inorganic phosphate in plants with cellular and subcellular resolution. *Plant Physiol* **167**(3), 628–638.

Muller, S.M., Galliardt, H., Schneider, J., Barisas, B.G. & Seidel, T. (2013). Quantification of Forster resonance energy transfer by monitoring sensitized emission in living plant cells. *Front Plant Sci* **4**, 413. doi:410.3389/fpls.2013.00413.

Murashige, T. & Skoog, F. (1962). A revised medium for rapid growth and bioassays with tobacco tissue cultures. *Physiologia Plantarum* **15**, 473–497.

Nagai, T., Yamada, S., Tominaga, T., Ichikawa, M. & Miyawaki, A. (2004). Expanded dynamic range of fluorescent indicators for Ca2+ by circularly permuted yellow fluorescent proteins. *Proc Natl Acad Sci USA* **101**(29), 10554–10559.

Okumoto, S. (2014). Quantitative imaging approaches for small-molecule measurements using FRET sensors in plants. *Methods Mol Biol* **1083**, 55–64.

Okumoto, S., Jones, A. & Frommer, W.B. (2012). Quantitative imaging with fluorescent biosensors. *Ann Rev Plant Biol* **63**, 663–706.

Plaxton, W.C. & Tran, H.T. (2011). Metabolic adaptations of phosphate-starved plants. *Plant Physiol* **156**(3), 1006–1015.

Pratt, J., Boisson, A.M., Gout, E., Bligny, R., Douce, R. & Aubert, S. (2009). Phosphate (Pi) starvation effect on the cytosolic Pi concentration and Pi exchanges across the tonoplast in plant cells: An in vivo 31P-nuclear magnetic resonance study using methylphosphonate as a Pi analog. *Plant Physiol* **151**(3), 1646–1657.

Raghothama, K. (1999). Phosphate acquisition. *Annu Rev Plant Physiol Plant Mol Biol* **50**, 665–693.

Rebeille, F., Bligny, R. & Douce, R. (1984). Is the cytosolic Pi concentration a limiting factor for plant cell respiration? *Plant Physiol* **74**(2), 355–359.

Rincon-Zachary, M., Teaster, N.D., Sparks, J.A., Valster, A.H., Motes, C.M. & Blancaflor, E.B. (2010). Fluorescence resonance energy transfer-sensitized emission of yellow cameleon 3.60 reveals root zone-specific calcium signatures in Arabidopsis in response to aluminum and other trivalent cations. *Plant Physiol* **152**(3), 1442–1458.

Roszik, J., Lisboa, D., Szollosi, J. & Vereb, G. (2009). Evaluation of intensity-based ratiometric FRET in image cytometry—Approaches and a software solution. *Cytometry A* **75**(9), 761–767.

Shaner, N.C., Steinbach, P.A. & Tsien, R.Y. (2005). A guide to choosing fluorescent proteins. *Nat Methods* **2**(12), 905–909.

Sharkey, T.D. & Vanderveer, P.J. (1989). Stromal phosphate concentration is low during feedback limited photosynthesis. *Plant Physiol* **91**(2), 679–684.

van Rheenen, J., Langeslag, M. & Jalink, K. (2004). Correcting confocal acquisition to optimize imaging of fluorescence resonance energy transfer by sensitized emission. *Biophys J* **86**(4), 2517–2529.

Vance, C.P., Uhde-Stone, C. & Allan, D.L. (2003). Phosphorus acquisition and use: Critical adaptations by plants for securing a nonrenewable resource. *New Phytol* **157**, 423–447.

Waadt, R., Hitomi, K., Nishimura, N., Hitomi, C., Adams, S.R., Getzoff, E.D. & Schroeder, J.I. (2014). FRET-based reporters for the direct visualization of abscisic acid concentration changes and distribution in Arabidopsis. *Elife* **3**, e01739.

Walker, D.A. & Sivak, M.N. (1986). Photosynthesis and phosphate: A cellular affair? *Trends Biochem Sci* **11**, 176–179.

Wallrabe, H. & Periasamy, A. (2005). Imaging protein molecules using FRET and FLIM microscopy. *Curr Opin Biotech* **16**(1), 19–27.

Xia, Z. & Liu, Y. (2001). Reliable and global measurement of fluorescence resonance energy transfer using fluorescence microscopes. *Biophys J* **81**(4), 2395–2402.

Yang, H., Bogner, M., Stierhof, Y.D. & Ludewig, U. (2010). H-independent glutamine transport in plant root tips. *PLoS One* **5**(1), e8917.

Zhang, Z., Liao, H. & Lucas, W.J. (2014). Molecular mechanisms underlying phosphate sensing, signaling, and adaptation in plants. *J Integr Plant Biol* **56**(3), 192–220.